JOURNAL OF AIRCRAFT
Vol. 34, No. 5, September–October 1997

Development of Closed-Loop Tail-Sizing Criteria for a High Speed Civil Transport

Isaac I. Kaminer* and Richard M. Howard†
Naval Postgraduate School, Monterey, California 93943
and
Carey S. Buttrill‡
NASA Langley Research Center, Hampton, Virginia 23681

A study was conducted to determine the closed-loop tail-sizing criteria for a High Speed Civil Transport using a newly developed integrated aircraft/controller design methodology. The key idea is to cast closed loop requirements as linear matrix inequalities, for which efficient numerical solvers are available. In particular, the effects of certain feedback specifications, and of actuator amplitude and rate constraints on the maximum allowable c.g. travel for a given set of tail sizes are studied. A constant gain state feedback controller is designed as a part of the tail-sizing process.

Nomenclature

a = actuator bandwidth, rad/s
$\bar{c}$ = mean aerodynamic chord
c_1, c_2 = constants used to define conic sector in complex plane
$\mathcal{F}$ = aircraft equations of motion
$\mathcal{G}$ = nonlinear aircraft dynamics
$\mathcal{G}_l$ = linear aircraft dynamics
$\mathcal{H}$ = aircraft sensor output equations
l_t = tail length
S = wing area
S_t = horizontal tail area
u = tail incidence angle, deg
$u_{\max}$ = actuator amplitude limit, deg
$\dot{u}_{\max}$ = actuator rate limit, deg
V_H = $l_t S_t/\bar{c}S$, normalized horizontal tail volume
V_T = airspeed, ft/s
$\boldsymbol{x}$ = aircraft state vector
$\boldsymbol{x}_a$ = actuator state
$\boldsymbol{x}_{cg}$ = center of gravity
$\boldsymbol{x}(0)$ = initial condition
β = number used to define a half-plane region in the complex plane
γ = flight path angle, deg

I. Introduction

DESIGN difficulties arise for configurations spanning speed ranges from the subsonic approach condition to supersonic cruise. For the next-generation supersonic aircraft like High Speed Civil Transport (HSCT), the c.g. position may be optimized by fuel transfer to minimize drag and to compensate for the shift of the aerodynamic center during transonic flight. The HSCT will require stability augmentation for the unstable short-period mode related to the negative static margin during subsonic flight. Sizing the horizontal tail is no longer a simple task and must be related to the varying c.g. location and the ability to perform pitch recovery for the various flight phases.[1]

In airplane conceptual and preliminary design, the horizontal tail is typically sized according to static criteria. For a given tail volume V_H, constraints are calculated that limit the fore and aft travel of the c.g. Constraints that limit forward c.g. position include 1) sufficient nose-up pitch acceleration at a rotation speed (nose–wheel liftoff), 2) sufficient nose-up pitch acceleration at the approach speed in the landing configuration (go-around), and 3) at brake release with maximum thrust, sufficient weight on the nose gear (tip back). Constraints that limit aft c.g. position include 1) pitch-up acceleration at the rotation speed (nose–wheel liftoff), and 2) sufficient nose-down pitch acceleration at minimum flying speeds. When these calculations are repeated for different tail sizes, a scissors sizing plot is created (Fig. 1).

For unstable airplanes, the need to include dynamic considerations in the configuration definition process emerges. References 2 and 3 describe early published work by Beaufrere in this area, largely motivated by the X-29 research program. Schmidt[4] uses the system sensitivity function to describe the fundamental tradeoff that exists between the level of static instability that can be controlled and vehicle flexibility.

Previous (unpublished) work in industry relied on time-domain analysis to determine, for a given design gust disturbance and a given rate and position limits of the pitch control effector, how far aft (how unstable) could the c.g. be before the airplane becomes unrecoverable. The analysis was somewhat unconservative in that the control effector moved instantly in the right direction at maximum rate to effect recovery. In a closed-loop stabilized vehicle, an error signal would have to build up before the effector reached the rate limit, and the effector would in-effect get a late start.

The main objective of the work in this paper is to include the effects of feedback and certain flying qualities criteria on the computation of aft c.g. limits that still allow vertical gust recovery. This paper builds on previous work[5] where an integrated aircraft controller design methodology using linear matrix inequalities was applied to the control power sizing for an F-14 aircraft. In Ref. 5, the authors considered a problem of minimizing the weighted sum of the areas of the aircraft's stabilator and spoiler surfaces subject to feedback performance requirements expressed as a bound on the $\mathcal{H}_\infty$ norm of a closed-loop transfer function. A similar approach is used in this paper to determine the maximum allowable c.g. travel for a given tail size. The key idea is to formulate a con-

Received May 28, 1996; revision received June 2, 1997; accepted for publication June 4, 1997.

*Assistant Professor, Department of Aeronautics and Astronautics, Code AA/Ka. Member AIAA.
†Associate Professor, Department of Aeronautics and Astronautics, Code AA/Ho. Senior Member AIAA.
‡Research Technologist, Dynamics and Control Branch, M/S 489. Senior Member AIAA.

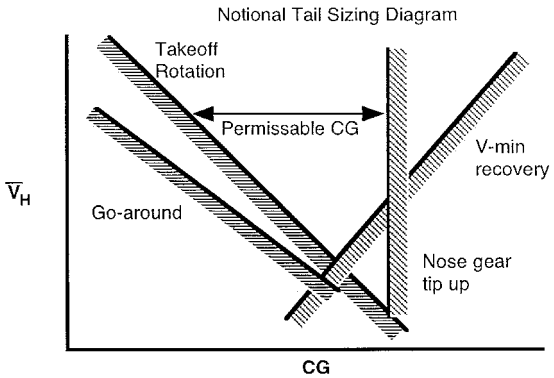

Fig. 1 Typical scissors sizing plot.

strained optimization problem where the cost J to be maximized is the aircraft's c.g. travel, and the search is done over a set of feedback controllers that guarantee internal stability, satisfy some specified MIL-STD 1797 levels I and II flying qualities requirements, and do not exceed actuator amplitude and rate constraints in response to a severe vertical gust.

In this paper, we show that the requirements discussed in the preceding text can be expressed as linear matrix inequalities (LMIs). LMIs have been used in systems and control for over a century. The first LMI can be attributed to Lyapunov, who showed that the differential equation $\dot{x} = Ax$ is stable if, and only if, the inequality $A^TP + PA \leq 0$ has a positive definite solution $P > 0$. The expressions $P > 0$ and $A^TP + PA \leq 0$ are LMIs. Since then, LMIs have been widely used to solve control system analysis and design problems. An interesting historical perspective on LMIs in systems and control can be found in Ref. 6. More recently, it has been shown that such well-known control problems such as $\mathcal{H}_2$ and $\mathcal{H}_\infty$ synthesis can also be formulated as LMIs (see Ref. 6 and the references therein).

This paper is organized as follows. Section II provides a brief introduction to LMIs and formulates the feedback stability, certain MIL-STD 1797 levels I and II flying qualities requirements as well as the actuator rate and amplitude constraints as LMIs. Section III formulates the proposed integrated c.g./controller synthesis problem as a constrained optimization problem (PCO: plant controller optimization). Section III introduces a numerical algorithm for solving the PCO and presents optimization history for several key parameters, including c.g., for a typical run of the algorithm. The complete set of results obtained using the algorithm can be found in Sec. IV. The aerodynamic model representative of an HSCT-like aircraft was used to obtain the numerical results in Sec. IV. It was developed from basic trim data for the supersonic B-70 aircraft,[7] suitably modified by the addition of a conventional aft tail using the specifications of Ref. 1. Other HSCT models are available in the literature.[8,9] The paper ends with some conclusions.

II. Background: Linear Matrix Inequalities

A detailed discussion of linear matrix inequalities and of their use in systems and control can be found in a book by Boyd et al.[6] In this section, we introduce some of the definitions in Ref. 6 and develop the LMIs necessary for the problem at hand.

Consider the expression:

$$F(\boldsymbol{x}) = F_0 + \sum_{i=1}^{p} \boldsymbol{x}_i F_i \geq 0 \tag{1}$$

where $\boldsymbol{x} \in \mathcal{R}^p$ is called a decision vector, and the matrices F_i are symmetric: $F_i = F_i^T \in \mathcal{R}^{n\times n}$. Expression (1) is a linear matrix inequality (LMI) because it exhibits linear dependence on the decision vector $\boldsymbol{x}$. The matrix $F(\boldsymbol{x})$ is positive semidefinite, i.e., $y^TF(\boldsymbol{x})y \geq 0\ \forall\ y \in \mathcal{R}^n$. A collection of LMIs $[F_1(\boldsymbol{x}) \geq 0, \ldots \boldsymbol{F}_k(\boldsymbol{x}) \geq 0]$ can be reduced to a single LMI by diagonally stacking each element: $\text{diag}[F_1(\boldsymbol{x}), \ldots F_k(\boldsymbol{x})] \geq 0$. Henceforth, the expression solving a given LMI will mean finding a decision vector $\boldsymbol{x}$ that makes the matrix $F(\boldsymbol{x})$ positive semidefinite.

Consider the Lyapunov inequality, $A^TP + PA \leq 0$, $P > 0$ discussed in Sec. I. Define a set of symmetric matrices $\mathcal{P} = [P_i = P_i^T \in \mathcal{R}^{n\times n},\ 1 \leq i \leq n(n+1)/2]$. Each matrix $P_i \in \mathcal{P}$ has the following form: the (i, i)th element of P_i is set to $1 \leq i \leq n$, and the rest of its entries are 0, whereas for $n+1 \leq i \leq n(n+1)/2$, P_i has two ones located symmetrically about the diagonal and the rest of its entries are 0. For example, let $n = 4$, then

$$P_2 = \begin{bmatrix} 0 & 0 & 0 & 0 \\ 0 & 1 & 0 & 0 \\ 0 & 0 & 0 & 0 \\ 0 & 0 & 0 & 0 \end{bmatrix}, \qquad P_5 = \begin{bmatrix} 0 & 1 & 0 & 0 \\ 1 & 0 & 0 & 0 \\ 0 & 0 & 0 & 0 \\ 0 & 0 & 0 & 0 \end{bmatrix}$$

Clearly, the set $\mathcal{P}$ forms a basis for a space of $n \times n$ symmetric matrices. Therefore, the solution to the Lyapunov inequality P can be expressed as

$$P = \sum_{i=1}^{n(n+1)/2} \boldsymbol{x}_i P_i$$

where $\boldsymbol{x}_i$ is an element of a decision vector $\boldsymbol{x} \in \mathcal{R}^{n(n+1)/2}$. It follows that a solution to the Lyapunov inequality can be found by solving the inequalities

$$\sum_{i=1}^{n(n+1)/2} \boldsymbol{x}_i P_i > 0 \tag{2}$$

$$-\sum_{i=1}^{n(n+1)/2} \boldsymbol{x}_i A^T P_i - \sum_{i=1}^{n(n+1)/2} \boldsymbol{x}_i P_i A \geq 0 \tag{3}$$

for the decision vector $\boldsymbol{x}$. These expressions are in the form of the LMI (1). Following the steps outlined earlier, any matrix inequality that is linear in the matrix variables can be reduced to the form of expression (1). Therefore, when deriving LMIs, these steps are usually omitted.[6]

Efficient interior point numerical techniques for solving LMIs can be found in Refs. 6, 10, and 11. Mathworks recently released LMI-Lab (Ref. 12), a MATLAB toolbox that employs one of the interior point techniques, the so-called projective method.[11]

In this paper, we are interested in obtaining feedback controllers that stabilize the aircraft and do not exceed actuator amplitude and rate constraints in response to a severe vertical gust represented by an appropriate initial condition vector $x(0)$. Next, we present the LMI characterization of such state-feedback controllers. Consider a linear system

$$\begin{cases} \dot{\boldsymbol{x}} = A\boldsymbol{x} \\ z = C\boldsymbol{x} \end{cases} \tag{4}$$

where $\boldsymbol{x} \in \mathcal{R}^n$, $z \in \mathcal{R}^1$. Then, the absolute value of the output $|z(t)|$ does not exceed an upper bound $z_{\max}$ in response to an initial condition $\boldsymbol{x}(0)$, if the system of LMIs has a solution $P > 0$, (Ref. 6):

$$\begin{bmatrix} P & C^T \\ C & z_{\max}^2 \end{bmatrix} \geq 0, \qquad \boldsymbol{x}(0)^TP\boldsymbol{x}(0) \leq 1, \qquad A^TP + PA < 0 \tag{5}$$

Notice that for such P to exist, the matrix A must have all its eigenvalues in the open left-half plane. Expression (5) was used in Ref. 6 to obtain a sufficient condition for the existence

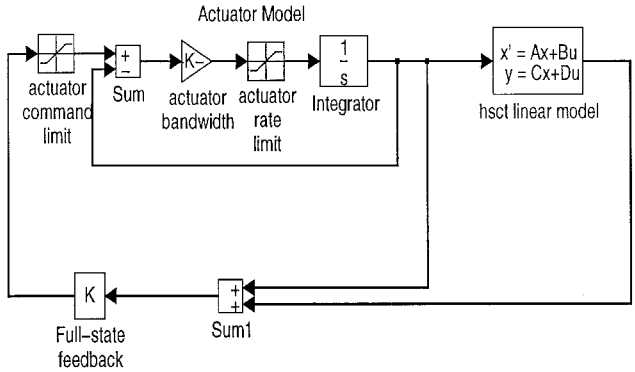

Fig. 2 Feedback system $\mathcal{G}_l$.

of a stabilizing constant gain state-feedback controller that would not exceed actuator amplitude constraint in response to a given initial condition $\boldsymbol{x}(0)$. This result is shown next.

Consider a feedback system

$$\mathcal{G} = \begin{cases} \dot{\boldsymbol{x}} = A\boldsymbol{x} + Bu \\ u = K\boldsymbol{x} \end{cases} = \begin{cases} \dot{\boldsymbol{x}} = (A + BK)\boldsymbol{x} \\ u = K\boldsymbol{x} \end{cases}$$

where $u \in R^1$ is the control input and $\mathcal{G}$ is in the form of expression (4). Suppose $\exists Y \in R^{n\times n}$, $Y > 0$, and $W \in R^{1\times n}$, such that

$$\begin{bmatrix} 1 & \boldsymbol{x}(0)^T \\ \boldsymbol{x}(0) & Y \end{bmatrix} \geq 0, \qquad \begin{bmatrix} Y & W^T \\ W & u_{\max}^2 \end{bmatrix} \geq 0$$
$$AY + BW + YA^T + BW^T < 0 \tag{6}$$

then $K = WY^{-1}$ is a constant state-feedback controller that stabilizes the feedback system $\mathcal{G}$ and meets actuator amplitude constraints in response to an initial condition $\boldsymbol{x}(0)$. Expressions (6) constitute an LMI in the matrix variables W and Y.

A similar approach yields an LMI characterization of the constant state-feedback controller that meets the actuator rate constraint in response to a given initial condition. First we need to append an actuator model to the aircraft. The actuator model is given by a first-order transfer function $a/(s + a)$ (Fig. 2). As a result, we obtain

$$\mathcal{G}_l = \begin{cases} \dot{\boldsymbol{x}} = A\boldsymbol{x} + B\boldsymbol{x}_a \\ \dot{\boldsymbol{x}}_a = -a\boldsymbol{x}_a + au \\ u = K[\boldsymbol{x} \quad \boldsymbol{x}_a]^T \\ \dot{\boldsymbol{x}}_a = -a\boldsymbol{x}_a + aK[\boldsymbol{x} \quad \boldsymbol{x}_a]^T \end{cases} = \begin{cases} \dot{\boldsymbol{v}} = (F + GK)\boldsymbol{v} \\ u = K\boldsymbol{v} \\ \dot{\boldsymbol{x}}_a = a(K - [0 \quad 1])\boldsymbol{v} \end{cases} \tag{7}$$

where $\boldsymbol{v} = [\boldsymbol{x} \quad \boldsymbol{x}_a]^T$

$$F = \begin{bmatrix} A & B \\ 0 & -a \end{bmatrix}, \qquad G = \begin{bmatrix} 0 \\ a \end{bmatrix}$$

and $\boldsymbol{x}_a$ and $\dot{\boldsymbol{x}}_a$ represent actuator position and rate, respectively. Notice, that in Eq. (7) we allowed for the feedback of $\boldsymbol{x}_a$. Now, following the steps in Ref. 6, we can derive a sufficient condition for the existence of a stabilizing state-feedback controller $K \in \mathcal{R}^{1\times(n+1)}$, which does not exceed a bound on $\boldsymbol{x}_a$ in response to an initial condition $\boldsymbol{x}(0)$. This can be done by applying expression (5) to the feedback system $\mathcal{G}_l$. Suppose, $\exists P > 0 \in \mathcal{R}^{(n+1)\times(n+1)}$ and $K \in \mathcal{R}^{1\times(n+1)}$, such that

$$\begin{bmatrix} P & a[K - [0 \quad 1]]^T \\ a[K - [0 \quad 1]] & u_{\max}^2 \end{bmatrix} \geq 0$$
$$\boldsymbol{x}(0)^T P \boldsymbol{x}(0) \leq 1, \qquad (F + GK)^T P + P(F + GK) < 0 \tag{8}$$

then $\mathcal{G}_l$ is internally stable, and $|\boldsymbol{x}_a(t)| < u_{\max}\ \forall\ t \geq 0$. The last expression in Eq. (8) is not linear in matrix variables K and P. Let $Y = P^{-1}$ and $W = KY$. Then

$$(F + GK)^T P + P(F + GK) < 0 \Leftrightarrow (F + GK)Y + Y(F + GK)^T < 0 \Leftrightarrow FY + GW + YF^T + GW^T < 0 \tag{9}$$

Now, expression (9) is linear in new matrix variables W and Y, and is, therefore, an LMI. Furthermore

$$\begin{bmatrix} P & a[K - [0 \quad 1]]^T \\ a[K - [0 \quad 1]] & u_{\max}^2 \end{bmatrix} \geq 0$$
$$\Leftrightarrow \begin{bmatrix} Y & 0 \\ 0 & I \end{bmatrix} \begin{bmatrix} P & a[K - [0 \quad 1]]^T \\ a[K - [0 \quad 1]] & u_{\max}^2 \end{bmatrix} \begin{bmatrix} Y & 0 \\ 0 & I \end{bmatrix} \geq 0 \Leftrightarrow \begin{bmatrix} Y & a[W - [0 \quad 1]Y]^T \\ a[W - [0 \quad 1]Y] & u_{\max}^2 \end{bmatrix} \geq 0 \tag{10}$$

Finally, using Schur complements[6] we get

$$x(0)^T P x(0) \leq 1 \Leftrightarrow \boldsymbol{x}(0)^T Y^{-1} \boldsymbol{x}(0) \leq 1 \Leftrightarrow \begin{bmatrix} 1 & \boldsymbol{x}(0)^T \\ \boldsymbol{x}(0) & Y \end{bmatrix} \geq 0 \tag{11}$$

Inequalities (9–11) are linear in Y and W. Moreover, if such Y and W exist, then the controller $K = WY^{-1}$ stabilizes $\mathcal{G}_l$ and does not exceed the actuator rate constraint $u_{\max}$.

By combining expressions (6, 9–11), we derive a sufficient condition for the existence of a stabilizing state-feedback gain K that satisfies actuator amplitude and rate constraints. Suppose $\exists W$ and $Y > 0$, such that

$$\begin{bmatrix} Y & a[W - [0 \quad 1]Y]^T \\ a[W - [0 \quad 1]Y] & u_{\max}^2 \end{bmatrix} \geq 0$$
$$\begin{bmatrix} 1 & \boldsymbol{x}(0)^T \\ \boldsymbol{x}(0) & Y \end{bmatrix} \geq 0, \qquad FY + GW + YF^T + GW^T < 0 \tag{12}$$
$$\begin{bmatrix} Y & W^T \\ W & u_{\max}^2 \end{bmatrix} \geq 0$$

then the controller $K = WY^{-1}$ stabilizes $\mathcal{G}_l$ and meets the actuator rate and amplitude constraints. We emphasize that the amplitude constraint is on the feedback controller command u rather than on the actuator position $\boldsymbol{x}_a$. Expression (12) represents an LMI and can be solved using standard LMI software.

So far, we considered controllers that only place eigenvalues of $\mathcal{G}_l$ in the open left-half plane. However, to achieve certain level I or II flying qualities requirements, the eigenvalues of $\mathcal{G}_l$ must be placed in more restrictive regions in the left-half plane. Figure 3 shows the bounded region that can be used to define suggested levels I and II category B closed-loop locations of the HSCT short-period mode for the flight condition used in this study. The bounded region provides acceptable short-period locations characterized by a minimum damping ratio of 0.3 and an undamped natural frequency of 0.3 rad/s. Level II requirements lower the minimum damping ratio to 0.2. Therefore, to meet either level I or II requirements for the HSCT, the short-period eigenvalues of the closed-loop system $\mathcal{G}_l$ must be placed in the following region in the complex plane (Fig. 3):

$$\mathcal{L} = [z \in \mathcal{C}: \mathrm{Re}(z) < -\beta, c_1\,\mathrm{Re}(z) + |c_2\,\mathrm{Im}(z)| < 0]$$

where $c_1 = \sin\phi$, $c_2 = \cos\phi$, and $\phi = \cos^{-1}\zeta$, and ζ denotes the desired minimum damping of the closed-loop poles. In their work, Gahinet and Chilali[13] introduced a concept of an LMI region and showed that such regions can be characterized by LMIs. In particular, the reqion $\mathcal{L}$ is an LMI region. By

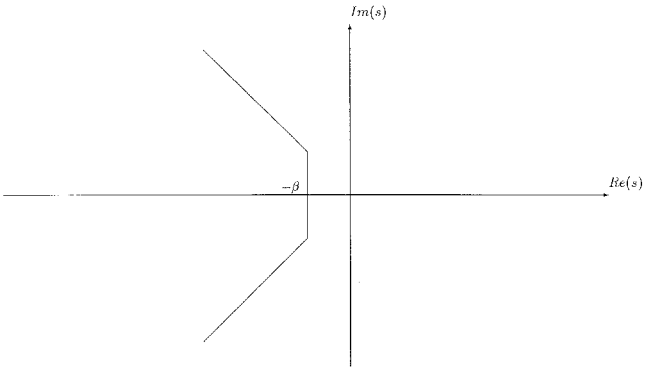

Fig. 3 Region $\mathcal{L}$ suggested MIL-STD 1797 locations for the short period.

applying the results in Ref. 13 to $\mathcal{G}_l$, we obtain a sufficient condition for the existence of a constant state-feedback controller that places the eigenvalues of $\mathcal{G}_l$ in the region $\mathcal{L}$. Suppose, $\exists Y \in \mathcal{R}^{(n+1)\times(n+1)}$ and $W \in \mathcal{R}^{1\times(n+1)}$ such that

$$\begin{bmatrix} c_1(FY+GW)+c_1(FY+GW)^T & -c_2(FY+GW)+c_2(FY+GW)^T & 0 \\ c_2(FY+GW)-c_2(FY+GW)^T & c_1(FY+GW)+c_1(FY+GW)^T & 0 \\ 0 & 0 & FY+GW+(FY+GW)^T+2\beta Y \end{bmatrix} < 0 \tag{13}$$

then the controller $K = WY^{-1}$ places the eigenvalues of $\mathcal{G}_l$ in $\mathcal{L}$. Therefore, by combining LMIs (12) and (13), we obtain a sufficient condition for the existence of a state-feedback controller K that satisfies the specified flying qualities requirements and meets the actuator amplitude and rate limit constraints.

III. Problem Formulation

The general problem addressed in this paper involves obtaining aft c.g. limits for a given HSCT flight condition and a set of horizontal tail volumes. In particular, we are interested in including specified flying quality requirements in the problem formulation. Therefore, the PCO problem to be solved in this paper can be stated as follows: For a given HSCT flight condition and V_H, find a maximum aft c.g. location and a state feedback controller that satisfy a particular set of flying quality requirements. Furthermore, the controller response to a vertical gust must not exceed prescribed actuator amplitude and rate constraints.

Let x_{cg} denote the c.g. location as a fraction of the reference chord, and let $\boldsymbol{x} \in \mathcal{R}^n$ be the vector of HSCT longitudinal states, and u denote the all-moving horizontal tail incidence angle. Then, the longitudinal dynamics of the aircraft can be expressed by the following system of differential equations:

$$\mathcal{G} = \begin{cases} \dot{\boldsymbol{x}} = \mathcal{F}(\boldsymbol{x}, u, \boldsymbol{x}_{cg}) \\ \boldsymbol{y} = \boldsymbol{x} \\ z = \mathcal{H}(\boldsymbol{x}) \end{cases} \tag{14}$$

where $\mathcal{F}(\,)$ is a continuously differentiable function of $\boldsymbol{x}$, u, and $\boldsymbol{x}_{cg}$, $\boldsymbol{y}$ is the vector of measured ouputs, and z is used to define the trim condition. Here, $z = [V_T \quad \gamma]^T$, and $\mathcal{H}$ is a continuously differentiable function of $\boldsymbol{x}$. Let $\boldsymbol{x}_0$, u_0 denote the trim values of $\boldsymbol{x}$ and u for a given z_0 and c.g. location $\boldsymbol{x}_{cg_0}$, i.e., $\mathcal{F}(\boldsymbol{x}_0, u_0, \boldsymbol{x}_{cg_0}) = 0$ and $\mathcal{H}(\boldsymbol{x}_0, u_0) = z_0$. In the sequel, when $\boldsymbol{x}_{cg}$ is allowed to change, the trim values $\boldsymbol{x}_0$ and u_0 will be recomputed for given values of $\boldsymbol{x}_{cg_0}$ and z_0. Now linearizing $\mathcal{G}$ about $\boldsymbol{x}_0$, u_0 yields the system of linear differential equations

$$\begin{cases} \delta\dot{\boldsymbol{x}} = A(z_0, \boldsymbol{x}_{cg_0})\delta\boldsymbol{x} + B(z_0, \boldsymbol{x}_{cg_0})\delta u \\ \delta y = \delta\boldsymbol{x} \end{cases} \tag{15}$$

where $\delta\boldsymbol{x}$, δu, and δy denote small perturbations of $\boldsymbol{x}$, u, and y about $\boldsymbol{x}_0$, u_0, and $y_0 = \boldsymbol{x}_0$, respectively. Following the development in Sec. II, we append the actuator model to Eq. (15) and denote the new system

$$\mathcal{G}_l(z_0, \boldsymbol{x}_{cg_0}) = \begin{cases} \dot{\boldsymbol{v}} = (F + GK)\boldsymbol{v} \\ \delta u = K\boldsymbol{v} \\ \boldsymbol{x}_a = a(K - [0 \quad 1])\boldsymbol{v} \end{cases} \tag{16}$$

where the definitions of F, G, and $\boldsymbol{v}$ can be easily determined by comparing Eq. (16) with Eq. (7). Figure 2 shows the diagram of the feedback system $\mathcal{G}_l(z_0, \boldsymbol{x}_{cg_0})$, which includes the location of actuator command and rate limits.

Define the set

$$\begin{aligned} &\Phi[\mathcal{G}_l(z_0, \boldsymbol{x}_{cg_0}), u_{max}, \dot{u}_{max}, \boldsymbol{x}(0)] \\ &= \left\{ W, Y: W \in \mathcal{R}^{1\times n}, Y \in \mathcal{R}^{n\times n}, Y > 0, \right. \\ &\begin{bmatrix} Y & a[W - [0 \quad 1]Y]^T \\ a[W - [0 \quad 1]Y] & \dot{u}_{max}^2 \end{bmatrix} \geq 0, \\ &\begin{bmatrix} 1 & \boldsymbol{x}(0)^T \\ \boldsymbol{x}(0) & Y \end{bmatrix} \geq 0, \quad FY + GW + YF^T + GW^T < 0, \\ &\left. \begin{bmatrix} Y & W^T \\ W & u_{max}^2 \end{bmatrix} \geq 0 \right\} \end{aligned} \tag{17}$$

where the LMIs used in the definition of Φ were derived in Sec. III. If set Φ is nonempty, then $K = WY^{-1}$ stabilizes $\mathcal{G}_l(z_0, \boldsymbol{x}_{cg_{00}})$ and does not exceed u_{max} and $\dot{u}_{max}$ in response to $\boldsymbol{x}(0)$. Based on the Federal Aviation Regulations gust loads formulation,[14] a derived equivalent gust velocity of 66 fps was used for the vertical gust $\boldsymbol{x}(0) = [0 \quad 66/V_T \quad 0 \quad 0]^T$. The first PCO problem considered in this paper can be stated as follows, given z_0:

Maximize $\{\boldsymbol{x}_{cg}\}$

Subject to:

$$\begin{aligned} &\mathcal{F}(\boldsymbol{x}_0, u_0, \boldsymbol{x}_{cg}) = 0 \\ &\mathcal{H}(\boldsymbol{x}_0, u_0) = z_0 \\ &(Y, W) \in \Phi[\mathcal{G}_l(z_0, \boldsymbol{x}_{cg}), u_{max}, \dot{u}_{max}, \boldsymbol{x}(0)] \end{aligned} \tag{18}$$

A solution to this PCO problem includes $K = WY^{-1}$, that stabilizes $\mathcal{G}_l(z_0, \boldsymbol{x}_{cg_0})$ and meets actuator limit requirements, as well as a maximum aft c.g. location.

A numerical solution used to solve the proposed PCO problem involves a binary search over $\boldsymbol{x}_{cg}$:

1. Fix V_H, V_T, γ. Let $\boldsymbol{x}_{cg_{max}} = 1$ and $\boldsymbol{x}_{cg_{min}} = 0$.
2. $\boldsymbol{x}_{cg_0} = (\boldsymbol{x}_{cg_{max}} + \boldsymbol{x}_{cg_{min}})/2$
3. Solve $\mathcal{F}(\boldsymbol{x}_0, u_0, \boldsymbol{x}_{cg_0}) = 0$, $\mathcal{H}(\boldsymbol{x}_0, u_0) = z_0$ for $\boldsymbol{x}_0$, u_0,
4. Obtain $A(\boldsymbol{x}_0, u_0, \boldsymbol{x}_{cg_0})$, $B(\boldsymbol{x}_0, u_0, \boldsymbol{x}_{cg_0})$ and form $\mathcal{G}_l(z_0, \boldsymbol{x}_{cg_0})$.

5. Solve for $(Y, W) \in \Phi(\mathcal{G}_l[z_0, \boldsymbol{x}_{cg_0}), u_{max}, \boldsymbol{u}_{max}, \boldsymbol{x}(0)]$
6. If no such (Y, W) exist
   - $\boldsymbol{x}_{cg_{max}} = \boldsymbol{x}_{cg_0}$

   else
   - $\boldsymbol{x}_{cg_{min}} = \boldsymbol{x}_{cg_0}$
7. If $\boldsymbol{x}_{cg_{max}} - \boldsymbol{x}_{cg_{min}} < tol$ exit
8. Go to 2

IV. Results

Figures 4–9 include an optimization history for a number of parameters during a typical run of the optimization algorithm. For this case, the value of the HSCT V_H is 0.4. Figure 4 shows the optimization history for c.g. Figures 5 and 6 include optimization histories for maximum actuator amplitude and rate deflections, respectively, of $\mathcal{G}_l(z_0, \boldsymbol{x}_{cg_0})$ in response to the vertical gust. Figures 7 and 8 depict the progress of the trim values of the angle of attack α_0 and of tail incidence angle U_0 as c.g. moves aft. Finally, Fig. 9 contains optimization history of the maximum eigenvalue of the LMIs (12). This eigenvalue must be negative for the constraint set Φ to be nonempty. Figure 9 clearly indicates that the controller K corresponding to the optimal c.g. is on the boundary of Φ.

To obtain a constant gain state-feedback controller that meets specified levels I and II handling quality requirements on $\mathcal{G}_l(z_0, \boldsymbol{x}_{cg_0})$, we redefine the set Φ in the optimization problem (18)

$$\Phi[\mathcal{G}_l(Z_0, \boldsymbol{x}_{cg_0}), u_{max}, \boldsymbol{u}_{max}, \boldsymbol{x}(0)] = \left\{ W, Y > 0: \begin{bmatrix} Y & a[W - [0 \quad 1]Y]^T \\ a[W - [0 \quad 1]Y] & \boldsymbol{u}_{max}^2 \end{bmatrix} \geq 0, \quad \begin{bmatrix} 1 & \boldsymbol{x}(0)^T \\ \boldsymbol{x}(0) & Y \end{bmatrix} \geq 0, \right.$$
$$\begin{bmatrix} c_1(FY + GW) + c_1(FY + GW)^T & -c_2(FY + GW) + c_2(FY + GW)^T & 0 \\ c_2(FY + GW) - b(FY + GW)^T & c_2(FY + GW) + c_1(FY + GW)^T & 0 \\ 0 & 0 & FY + GW + (FY + GW)^T + 2\beta Y \end{bmatrix} < 0,$$
$$\left. \begin{bmatrix} Y & W^T \\ W & u_{max}^2 \end{bmatrix} \geq 0 \right\}$$

where, for specified level I requirements, β was selected to be 0.2, and c_1 and c_2 were computed as follows. Using MIL-STD 1797, the minimum allowable level I damping ratio ζ for the HSCT short-period mode was determined to be 0.3. Therefore, based on the formulas introduced in Sec. II, we obtain $\phi = \cos^{-1}0.3$ and $c_1 = \sin\phi$ and $c_2 = \cos\phi$. Similarly, for level II requirements, we selected $\beta = 0.1$ and $\zeta = 0.2$. A solution to this PCO problem includes $K = WY^{-1}$ that satisfies specified levels I and II flying quality requirements and meets actuator limit constraints, as well as a maximum aft c.g. location.

The plant controller optimization problems introduced in Sec. III were solved for the following set of tail volumes {0.05, 0.1, 0.15, 0.2, 0.25, 0.3, 0.35, 0.4}. The resulting solutions were used to obtain a number of c.g. vs V_H scissor lines, each for a different set of requirements on K. These requirements include actuator amplitude and rate constraints in response to a vertical gust plus feedback stability and flying qualities specifications. In particular, such lines were generated for stability (closed-loop eigenvalues in the open left-half plane), specified levels I and II flying quality requirements (with actuator amplitude and rate constraints) (Table 1).

Figure 10 contains all of the c.g. vs V_H lines generated. Furthermore, to illustrate the benefits of using feedback to attain the desired flying qualities, we included a plot of the HSCT critical point. The critical point is defined as the c.g. location where the short period mode crosses the imaginary axis. Contrary to what might be expected, the critical point only slightly changes with tail volume. Clearly, the feedback controller produces significant improvements in the allowable c.g. travel for a fixed tail size. On the other hand, it allows for a large reduction in the size of the horizontal tail for a given c.g. location.

Figure 10 illustrates the tradeoffs inherent in imposing progressively more restrictive requirements on the feedback controller. The amount of maximum allowable c.g. travel for a fixed tail volume clearly decreases as the feedback specifications become more stringent. Moreover, the data presented in Fig. 10 can serve as a baseline for future work, where the benefits of using more sophisticated controllers can be investigated.

Figure 11 contains the closed-loop, short-period poles for each of the $(\boldsymbol{x}_{cg}, V_H)$ points in Fig. 10, corresponding to levels I and II and the basic stability plots. One can see that for the basic stability case, the closed-loop, short-period mode has essentially zero damping. On the other hand, the level II short-

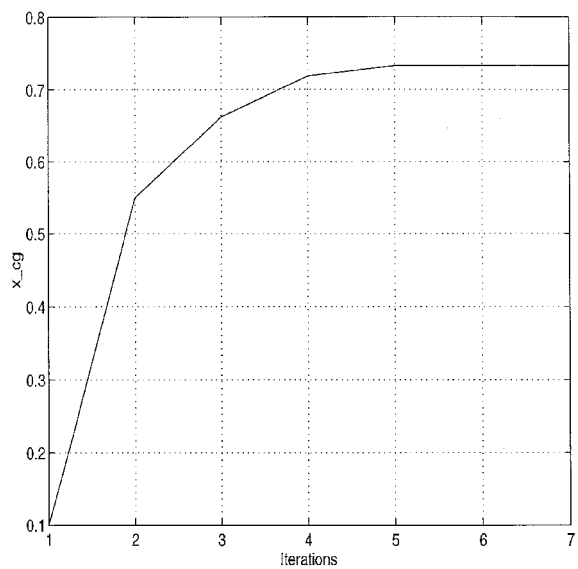

Fig. 4 Center of gravity optimization history.

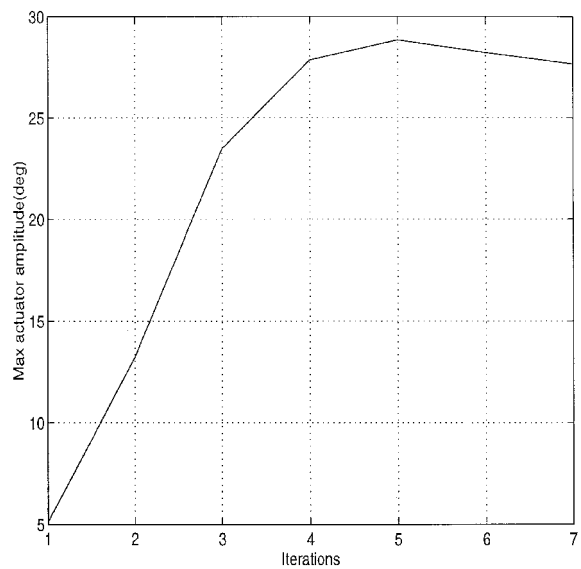

Fig. 5 Optimization history of maximum actuator deflection.

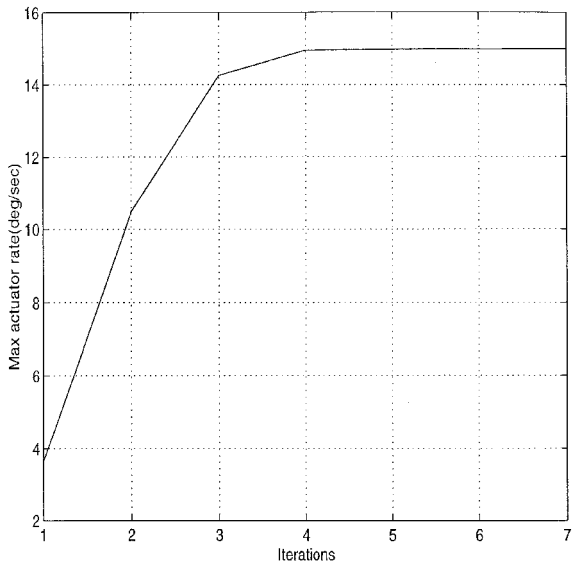

Fig. 6 Optimization history of maximum actuator rate deflection.

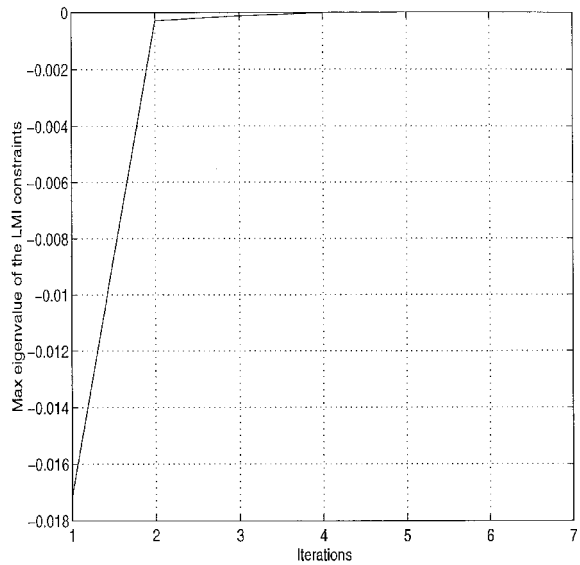

Fig. 9 Optimization history of max eigenvalue for constraint LMIs.

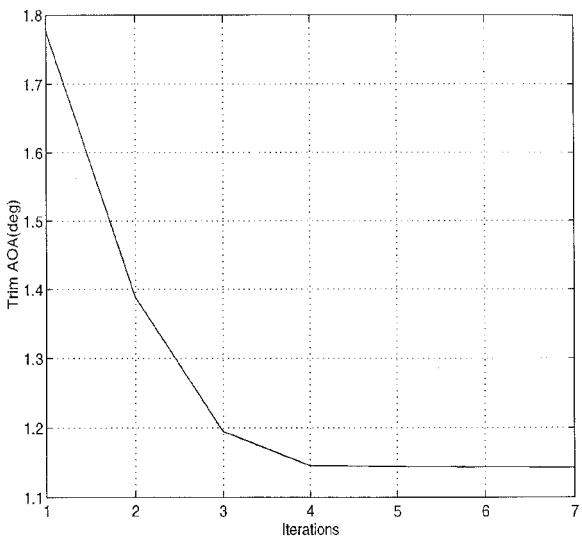

Fig. 7 Optimization history of trim α.

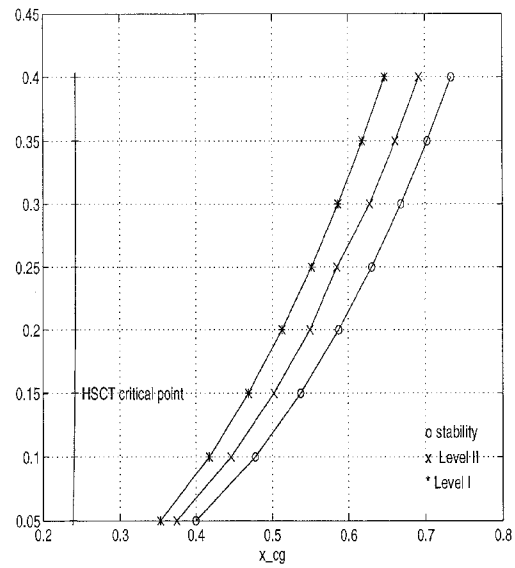

Fig. 10 Center of gravity vs V_H plots.

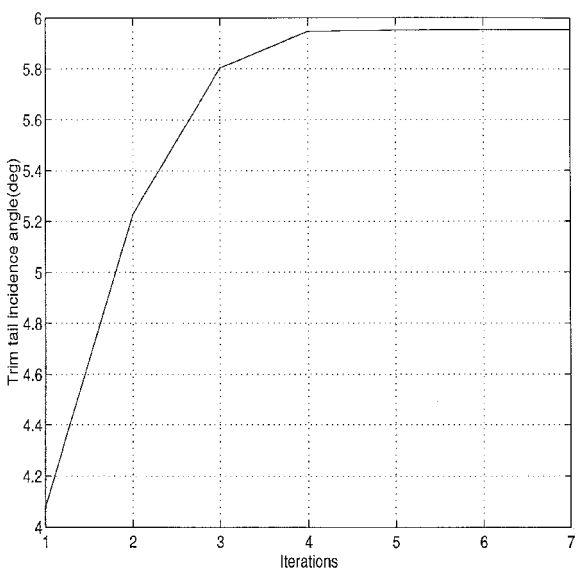

Fig. 8 Optimization history of trim tail incidence angle.

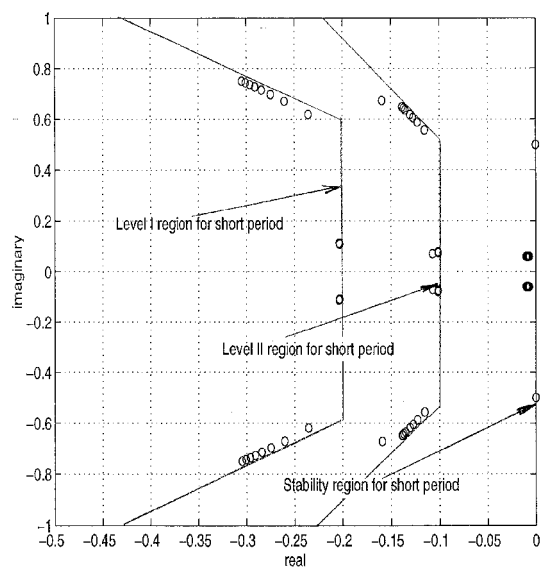

Fig. 11 Closed-loop eigenvalues for levels I and II and the basic stability cases.

Table 1 Summary of c.g. vs V_H lines generated

Line number	Stability	Level I	Level II	Act rate	Act amplitude
1	x			x	x
2		x		x	x
3			x	x	x

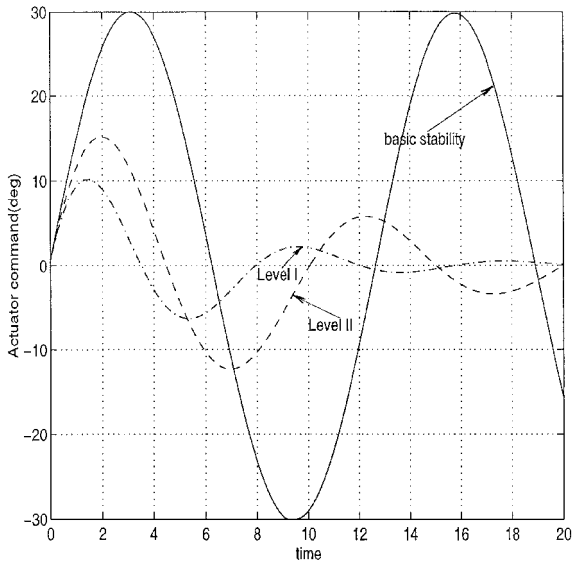

Fig. 12 Actuator command response to vertical gust.

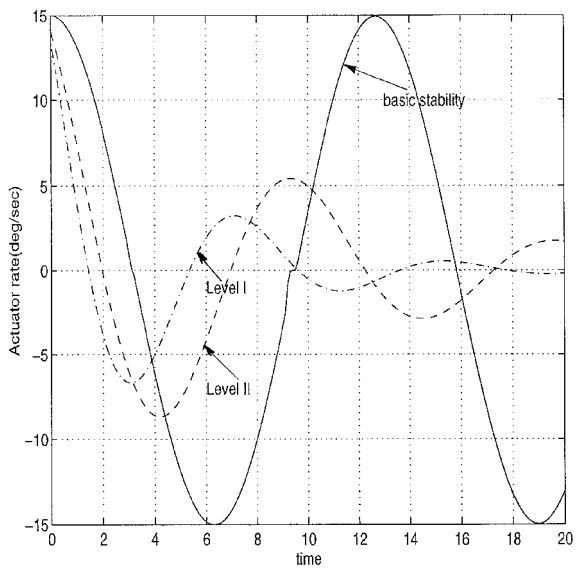

Fig. 13 Actuator rate response to vertical gust.

period mode has a damping ratio of 0.2, and the level I short-period mode a damping ratio of 0.3, as required.

Figures 12 and 13 include time histories of the responses of the tail control command and actuator rate to the vertical gust. In particular, for a fixed tail volume ($V_H = 0.15$), we show the response of levels I and II and the basic stability controllers. Clearly, the actuator response becomes better damped as the feedback requirements become more restrictive. Moreover, in Fig. 12, the basic stability controller moves the tail ± 30 deg. Because the trim tail value is 8 deg at this flight condition, the actuator command will reach the tail amplitude limit sooner than the linear response suggests. However, the response of levels II and I controllers will not exceed the amplitude limit when the tail trim setting is taken into account.

V. Conclusions

In this paper, we have introduced a nonlinear plant controller optimization problem that determines the maximum allowable c.g. travel for a given tail size for a high speed civil transport. The constraint set for this problem includes state-feedback controllers that satisfy flying qualities requirements as well as actuator amplitude and rate constraints. We have used linear matrix inequalities to obtain numerical solutions to the PCO problem. This paper demonstrated that the proposed optimization problem can be used to obtain quick answers to the critical issues involved in developing the tail sizing criteria for an HSCT-type aircraft.

The tools developed in this paper are intended for use in the early stages of aircraft design. They provide designers with an answer to the following fundamental question: Does a controller exist that can recover the aircraft from a severe gust without exceeding the actuator constraints for a given tail size and c.g. location? Therefore, the controllers produced by these tools are unlikely to be included in the final implementation of the aircraft's control system. However, they play an important role in assessing the limits of achievable performance. Finally, the LMIs used to obtain these controllers represent sufficient conditions for their existence. Therefore, the results obtained on c.g. travel using these LMI-based tools may be conservative.

Acknowledgments

This work was supported, in part, by the NASA/ASEE 1995 Summer Fellowship Program and by NASA Langley Research Center, Contract L65444D. The first author would like to thank David Christhilf of the Lockheed Martin Corporation for many insightful and helpful suggestions.

References

[1]Ray, J. K., Carlin, C. M., and Lambregts, A. A., "High-Speed Civil Transport Flight- and Propulsion-Control Technologies Issues," NASA CR 186015, March 1992.

[2]Beaufrere, H., and Soeder, S., "Longitudinal Control Requirements for Statically Unstable Aircraft," *Proceedings of the National Aerospace and Electronics Conference* (Dayton, OH), Vol. 2, A87-16726 05-01, Inst. of Electrical and Electronics Engineers, New York, 1986, pp. 421–433.

[3]Beaufrere, H., "Limitations of Statically Unstable Aircraft due to the Effects of Sensor Noise, Turbulence, and Structural Dynamics," *Proceedings of the AIAA Guidance, Navigation and Control Conference* (Williamsburg, VA), AIAA, New York, 1986, pp. 721–731.

[4]Schmidt, D. K., "On the Integrated Control of Flexible Supersonic Transport Aircraft," *Proceedings of the AIAA Guidance, Navigation and Control Conference* (Baltimore, MD), AIAA, Washington, DC, 1995, pp. 258–265.

[5]Niewhoener, R. J., and Kaminer, I., "On Integrated Aircraft/Controller Design Using Linear Matrix Inequalities," *Journal of Guidance, Control, and Dynamics*, Vol. 19, No. 2, 1996, pp. 445–453.

[6]Boyd, S., El Ghaoui, L., Feron, E., and Balakrishan, V., *Linear Matrix Inequalities in Systems and Control Theory*, SIAM, Philadelphia, PA, 1994.

[7]Ashley, H., *Engineering Analysis of Flight Vehicles*, Addison–Wesley, Reading, MA, 1974.

[8]Livne, E., Sels, R. A., Bhatia, K. G., "Lessons from Application of Equivalent Plate Structural Modeling to an HSCT Wing," *Journal of Aircraft*, Vol. 31, No. 4, 1994, pp. 953–960.

[9]Messac, A., and Hattis, P. D., "Physical Programming Design Optimization for High Speed Civil Transport," *Journal of Aircraft*, Vol. 33, No. 2, 1996, pp. 446–449.

[10]Gahinet, P., and Nemirovskii, A., "General Purpose LMI Solvers with Benchmarks," *Proceedings of the 32nd IEEE Conference on Decision and Control* (San Antonio, TX), Inst. of Electrical and Electronics Engineers, New York, 1993, pp. 3162–3165.

[11]Nemirovskii, A., and Gahinet, P., "The Projective Method for Solving Linear Matrix Inequalities," *Proceedings of the 1994 American Control Conference* (Baltimore, MD), IEEE Service Center, Piscataway, NJ, 1994, pp. 840–844.

[12]Gahinet, P., Nemirovski, A., Laub, A. J., and Chilali, M., *LMI Control Toolbox*, The Mathworks Inc., Natick, MA, 1995.

[13]Chilali, M., and Gahinet., P., "$\mathcal{H}_\infty$ Design with Pole Placement Constraints," *IEEE Transactions on Automatic Control*, Vol. 41, No. 3, 1996, pp. 358–367.

[14]Hoblit, F. M., *Gust Loads on Aircraft: Concepts and Applications*, AIAA Education Series, AIAA, Washington, DC, 1988, pp. 8, 9.